Environmental Science & Technology

Article

pubs.acs.org/est

Photodynamic Inactivation of Bacteria Using Novel Electrogenerated Porphyrin-Fullerene C_{60} Polymeric Films

M. Belén Ballatore, Javier Durantini, Natalia S. Gsponer, María B. Suarez, Miguel Gervaldo, Luis Otero, Mariana B. Spesia, M. Elisa Milanesio, and Edgardo N. Durantini*

Departamento de Química, Facultad de Ciencias Exactas Físico-Químicas y Naturales, Universidad Nacional de Río Cuarto, Agencia Postal Nro 3, X5804BYA Río Cuarto, Córdoba, Argentina

Supporting Information

ABSTRACT: A porphyrin-fullerene C_{60} dyad (TCP-C_{60}) substituted by carbazoyl groups was used to obtain electrogenerated polymeric films on optically transparent indium tin oxide (ITO) electrodes. This approach produced stable and reproducible polymers, holding fullerene units. The properties of this film were compared with those formed by layers of TCP/TCP-C_{60} and TCP/ZnTCP. Absorption spectra of the films presented the Soret and Q bands of the corresponding porphyrins. The TCP-C_{60} film produced a high photodecomposition of 2,2-(anthracene-9,10-diyl)bis-(methylmalonate), which was used to detect singlet molecular oxygen $O_2(^1\Delta_g)$ production in water. In addition, the TCP-C_{60} film induced the reduction of nitro blue tetrazolium to diformazan in the presence of NADH, indicating the formation of superoxide anion radical. Moreover, photooxidation of L-tryptophan mediated by TCP-C_{60} films was found in water. In biological media, photoinactivation of *Staphylococcus aureus* was evaluated depositing a drop with 2.5×10^3 cells on the films. After 30 min irradiation, no colony formation was detected using TCP-C_{60} or TCP/TCP-C_{60} films. Furthermore, photocytotoxic activity was observed in cell suspensions of *S. aureus* and *Escherichia coli*. The irradiated TCP-C_{60} film produced a 4 log decrease of *S. aureus* survival after 30 min. Also, a 4 log reduction of *E. coli* viability was obtained using the TCP-C_{60} film after 60 min irradiation. Therefore, the TCP-C_{60} film is an interesting and versatile photodynamic active surface to eradicate bacteria.

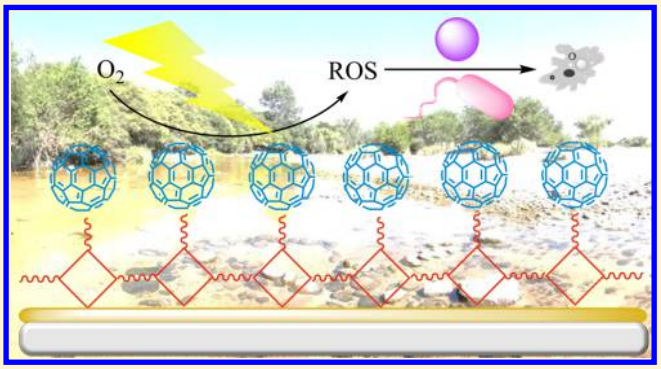

INTRODUCTION

Antibacterial resistance has increased dramatically over the past few years and is currently recognized as a major medical challenge in most healthcare settings.[1] With the development of society and technology over the last few decades, several factors have shifted the balance toward the emergence and uncontrolled spread of resistance. In addition to the gradually increasing consumption of antibiotics to treat illnesses, the utilization of these compounds as growth promoters in livestock production and the uncontrolled release of antibacterial substances into the environment have increased the selection pressure. Therefore, it is imperative to provide perspectives for the future prophylaxis or new treatments for bacterial infections.[2] In this way, photodynamic inactivation (PDI) of microorganisms has been projected as an alternative to controlling bacterial infections.[3] This approach combines a photosensitizer, visible light and oxygen to yield highly reactive oxygen species (ROS) that react with a variety of substrates generating damages in the biomolecules. These changes produce a loss of biological functionality, which leads to cell inactivation.

Most of the PDI studies have been carried out adding the photosensitizer to cell suspensions. In this procedure, after treatment traces of the photosensitizer can remain in the medium, leading to an undesired remnant photodynamic effect. An alternative to avoid this inconvenience is represented by light-activated antimicrobial surfaces. These surfaces kill microbes by the action of light and have potential applications in domestic and healthcare settings.[4] In healthcare environments, surfaces have been accepted as potential reservoirs of bacteria, which are associated with the incidence of nosocomial infection.[5] The transmission of bacteria, such as methicillin-resistant *Staphylococcus aureus*, between healthcare personnel and patients can result in morbidity in a hospital with immunocompromised patients.[6] To prevent the spread of nosocomial infection through direct contact, these microbial reservoirs need to be targeted. Consequently, the development of antimicrobial coatings for surfaces plays an important role in decreasing the incidence of nosocomial infection.

Several porphyrin-based compounds have demonstrated the photosensitization of pathogenic microorganisms upon visible

Received: April 2, 2015
Revised: May 11, 2015
Accepted: May 18, 2015
Published: May 18, 2015

DOI: 10.1021/acs.est.5b01407
Environ. Sci. Technol. 2015, 49, 7456−7463

light irradiation.[3] Recently, a carbazoyl porphyrin derivative was attached to fullerene C_{60} forming a novel porphyrin-fullerene C_{60} dyad (TCP-C_{60}, Figure 1).[7] This dyad has a porphyrin

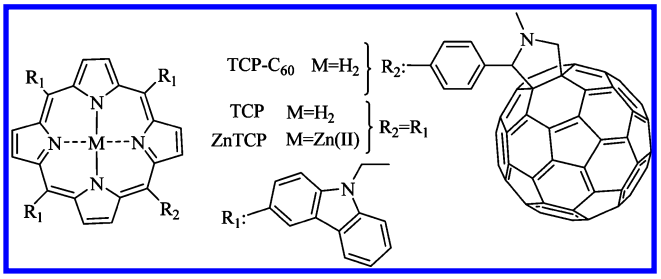

Figure 1. Molecular structures of carbazoyl porphyrin derivatives.

moiety that acts as light-harvesting antenna increasing visible light absorption. Also, it presents higher capacity to form a photoinduced charge-separated state, and the electron transfer process competes with the $O_2(^1\Delta_g)$ production. Thus, depending on the polarity of the microenvironment, porphyrin-fullerene C_{60} dyads can produce a biological photodamage through either a $O_2(^1\Delta_g)$-mediated photoreaction process or a free radical mechanism.[8]

Solid supported fullerene materials have been prepared with aims of creating a fullerene-based photoactive surface that is capable of producing ROS in the aqueous media.[9] Thus, in order to advance the potential of C_{60} as a photosensitizer in water systems, we propose an appropriated method of producing supported fullerene C_{60} materials. This approach is based on that porphyrins containing carbazoyl substituents are able to form electrodeposited layers by cyclic voltammetry.[10−12] Therefore, in the present study we used a TCP-C_{60} dyad to obtain electrogenerated polymeric films by cyclic voltammetry at oxidation potentials on optically transparent indium tin oxide (ITO) electrodes. Also, different layers of photosensitizers were combined to evaluate their photoinactivation capacities. Thus, polymeric films were formed from the carbazoyl porphyrin, TCP, and its metal complex with Zn(II), ZnTCP (Figure 1). The spectroscopic and photodynamic properties of these films were studied in water. Photodynamic action of the resultant modified materials was investigated *in vitro* to inactivate bacteria and determinate their effectivities as self-sterilizing agents activated by visible light.

EXPERIMENTAL SECTION

Reagents and Instrumentation. Chemicals from Aldrich (Milwaukee, WI, USA) were used without further purification. Tetrasodium 2,2′-(anthracene-9,10-diyl)bis(methylmalonate) (ABMM) was prepared as previously described.[13] Solvents (GR grade) from Merck (Darmstadt, Germany) were distilled. Ultrapure water was obtained from a Labconco (Kansas, MO, USA) equipment model 90901-01.

Absorption spectra were performed on a Shimadzu UV-2401PC spectrometer (Shimadzu Corporation, Tokyo, Japan). Fluorescence spectra were carried out on a Spex FluoroMax spectrofluorometer (Horiba Jobin Yvon Inc., Edison, NJ, USA). Fluence rates were determined with a Radiometer Laser Mate-Q (Coherent, Santa Clara, CA, USA). The visible light source used to irradiate solutions in 1 cm path length quartz cell was a Cole-Parmer illuminator 41720-series (Cole-Parmer, Vernon Hills, IL, USA) with a 150 W halogen lamp. Optical filters were used to select a wavelength range between 455 and 800 nm (44 mW/cm^2). Cell suspensions were irradiated with a Novamat 130 AF (Braun Photo Technik, Nürnberg, Germany) slide projector containing a 150 W lamp. A 2.5 cm glass cuvette filled with water was used to remove the heat from the lamp. A wavelength range between 350 and 800 nm was selected by optical filters (90 mW/cm^2).

Photosensitizers. 5,10,15,20-Tetrakis(4-sulfonatophenyl)-porphyrin sodium salt ($TPPS^{4-}$) was purchased from Aldrich. Chemical structures of carbazoyl porphyrin derivatives are shown in Figure 1. 5,10,15,20-Tetrakis[3-(*N*-ethylcarbazoyl)]-porphyrin (TCP) and TCP-C_{60} were synthesized as previously described.[7] This porphyrin was prepared from TCP (see the Supporting Information).

Electrochemical Experiments. Electrochemical experiments were performed at room temperature using *o*-dichlorobenzene (*o*-DCB) or 1,2-dichloroethane (DCE) solutions containing 0.1 M tetra-*n*-butylammonium perchlorate (TBAP) as supporting electrolyte, in a conventional three electrode cell. Cyclic voltammetry (CV) was carried out with an AUTOLAB PGSTAT30 potentiostat/galvanostat (Eco Chemie B. V., Utrecht, The Netherlands). Monomer and film characterizations were conducted using a Pt disc, a Pt foil, and a silver wire as working, counter, and pseudoreference electrodes, respectively. Also, ITO electrodes (7 × 50 × 0.9 mm, Delta Technologies, Stillwater, MN) were used as working electrodes in the formation of the single and double layer films. CVs were obtained at a scan rate of 100 mV/s.

Steady State Photolysis. Solutions of ABMM (35 μM) or L-tryptophan (Trp, 25 μM) in water (2 mL) containing the porphyrin $TPPS^{4-}$ or ITO electrodes with the electropolymeric film (Soret band, absorbance 0.1) were irradiated in a 1 cm path length quartz cell. The kinetics of ABMM and Trp photooxidation were studied following the decrease of the absorbance (A) at λ_{max} = 379 nm and the fluorescence intensity (I) at λ_{max} = 352 nm, respectively. The observed rate constants (k_{obs}) were obtained by a linear least-squares fit of the semilogarithmic plot of Ln A_0/A or I_0/I vs time.

Detection of Superoxide Anion Radical. The nitro blue tetrazolium (NBT) method was used to detect superoxide anion radical ($O_2^{\bullet-}$) formation in water.[14] This procedure was carried out using 0.2 mM NBT, 0.5 mM NADH, and $TPPS^{4-}$ or ITO electrodes with the electropolymeric film (Soret band, absorbance 0.1). Control experiments were performed in the absence of NBT, NADH, or photosensitizer. Samples (2 mL) were irradiated in 1 cm path length quartz cells under aerobic condition as described above. The progress of the reaction was observed by following the increase of the absorbance at λ = 600 nm.

Bacterial Strains and Preparation of Cultures. *S. aureus* ATCC 25923 and *Escherichia coli* EC7 strains were handled as previously described.[7,15] Viable bacteria were monitored, and the number of colony forming unit (CFU) was determined on tryptic soy (TS) agar plates after ∼24 h incubation at 37 °C.

Photoinactivation of Bacterial Cells on the Film Surface. For the antibacterial drop-test each film (0.7 × 3.0 = 2 .1 cm^2) was placed into a sterile Petri dish. Then, a droplet (250 μL) of the diluted saline solution containing *S. aureus* (∼10^4 CFU/mL) was placed on the surface of the film. The films were exposed to visible light for different time intervals. After that, cell suspensions were serially diluted with PBS, and colonies formed were counted.

Photosensitized Inactivation of Bacterial Cells Suspensions. Cell suspensions of *S. aureus* or *E. coli* (150 μL per

DOI: 10.1021/acs.est.5b01407
Environ. Sci. Technol. 2015, 49, 7456−7463

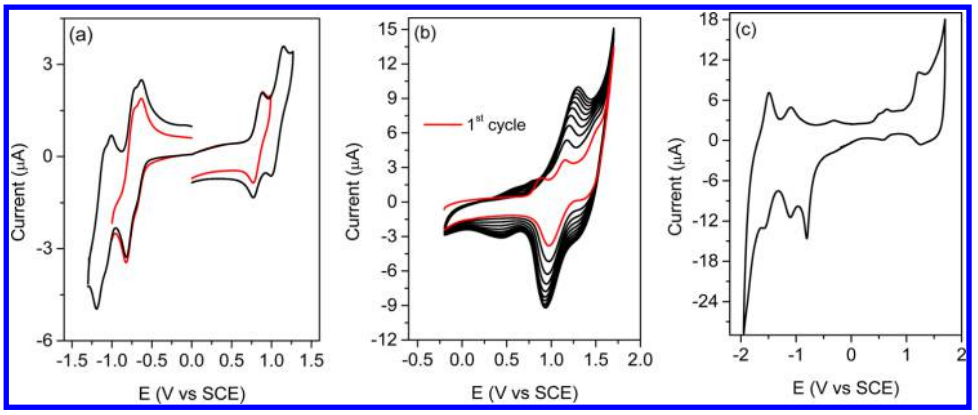

Figure 2. (a) First anodic and cathodic scans of TCP-C_{60} at different inversion potentials and (b) ten CV scans recorded in *o*-DCB containing TBAP using a Pt working electrode. (c) CV response of the film in DCE containing only a support electrolyte. Red lines after deposition of the first layer. Pt working electrode. All the CVs were obtained at a scan rate of 100 mV/s.

well, ~10^4 CFU/mL) in PBS were transferred to 96-well microtiter plates (Deltalab, Barcelona, Spain). To each well were added two small polymeric surfaces of the ITO electrode bearing the film (0.3 × 0.3 = 0.09 cm^2). Then the cell suspensions were exposed for different time intervals to visible light. Then, cell suspensions were serially diluted with PBS, and colonies were counted.

Controls and Statistical Analysis. Control experiments were performed in the presence and absence of polymer in the dark and in the absence of polymer with cells irradiated. Three values were obtained per each condition, and each experiment was repeated separately three times. The unpaired *t*-test was used to establish the significance of differences between groups. Differences were considered statistically significant with a confidence level of 95% ($p < 0.05$).

RESULTS AND DISCUSSION

Electrogenerated Polymeric Film Formation. Cyclic voltammetry was used in the generation of the different photoinactivating surfaces. Figure 2a shows cyclic voltammograms of TCP-C_{60} using a Pt electrode at different inversion potentials in the *o*-DCB-TBAP electrolyte. As it can be seen, the first two oxidation processes are reversible, and no changes in the faradaic currents are observed during continuous cycling, only the currents having been affected by diffusion. The first and second reversible oxidation processes can be attributed to the generation of the radical cation and dication in the tetrapyrrolic macrocyle, as is commonly observed in these type of conjugated centers.[16] However, the reduction process is more complex, where a series of overlapped waves are generated during the potential scan. In TCP-C_{60} both moieties, porphyrin and fullerene, can be reversibly reduced producing the observed voltammetric response (Figure 2a). This behavior is typical of this kind of dyad structures and has been well documented.[17] On the other hand, when the applied potential in the anodic scan is extended to 1.7 V a third oxidative process occurs, and a continuous increment in the faradaic currents is evidenced when successive voltammetric cycles are applied (Figure 2b). These increments are due to the growing of a conducting polymeric film on the electrode surface, formed by the coupling of carbazole radical cations, as it was demonstrated for similar substituted carbazole containing porphyrins.[10,11] Furthermore, when the Pt working electrode is removed from the TCP-C_{60} solution and positioned in an electrochemical cell containing only DCE-support electrolyte solution, it undergoes a surface oxidation−reduction process (Figure 2c) confirming that an electroactive product has been adsorbed on the electrode. A similar electropolymerization can be done on semitransparent ITO electrodes, allowing light absorption spectroscopic analysis and photoinactivation experiments with the formed films (vide infra). The observed electrochemical behavior could be explained taking into account that TCP-C_{60} has three carbazole units, besides the C_{60} group. It is known that oxidation of carbazole leads to the dimerization of two radical cations through the 3,3′ positions.[10] Thus, each TCP-C_{60} molecule can form trimers and/or tetramers, whose extension drives to the generation of a functional polymer absorbed on the electrode surface. An idealized polymer structure is shown in Figure S2a together with a AM1 optimized geometrical structure in Figure S2b. The homogeneous distribution of the TCP-C_{60} film on an ITO electrode is shown in Figure S3.

The TCP-C_{60} layer can be also grown on a previously electrodeposited TCP polymeric film,[10] i.e. a composite polymeric bilayer is formed: first a layer of TCP polymer and a second one of TCP-C_{60}. Figure S1a shows the voltammetric responses of the TCP electropolymer (red line) after ten cycles of electrodeposition and the corresponding TCP/TCP-C_{60} bilayer after ten cycles of TCP-C_{60} electropolymerization on the top of the TCP polymer film (black line). The CV shape of the first TCP layer is similar to that reported before,[10] while the bilayer presents contributions to the oxidation−reduction faradaic currents from both layers. In the same way, TCP/ZnTCP bilayers were formed by electrodeposition of a first layer of TCP and a second one of ZnTCP.[12,18] As it can be seen in Figure S1b, formation of the second layer of ZnTCP produces an increase in the oxidation/reduction currents of the film (with respect to that observed for the first layer) when it is placed in a solution containing only a support electrolyte. This observation confirms the deposition of ZnTCP. Similar electroactive layers were proposed for the construction of multicomponent supramolecular architectures suitable for efficient generation of surface photovoltages.[12,18]

Absorption Spectroscopic Properties. In a solution of *N*,*N*-dimethylformamide (DMF), the free-base TCP porphyrin presented a Soret band at 432 nm and four Q bands at 524, 563, 600, and 655 nm, while the corresponding ZnTCP derivatives showed a Soret band at 437 nm and two Q bands at around 564 and 607 nm (Figure 3a). In the visible region, the absorption spectrum of the TCP-C_{60} dyad is very similar to that

DOI: 10.1021/acs.est.5b01407
Environ. Sci. Technol. 2015, 49, 7456−7463

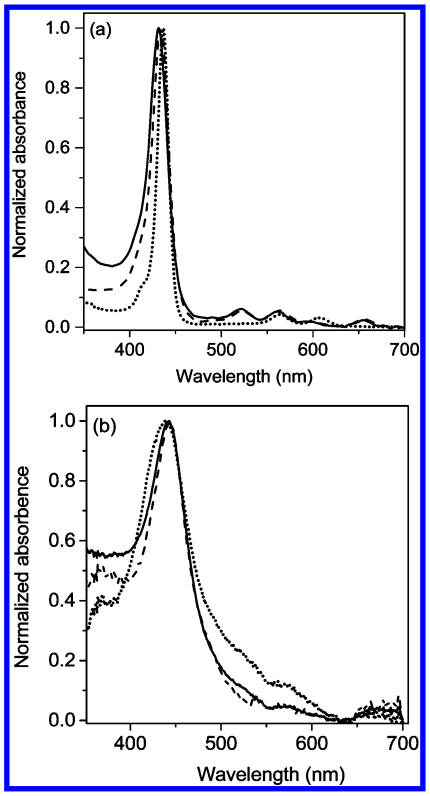

Figure 3. (a) Absorption spectra of TCP-C_{60} (solid line), TCP (dashed line), and ZnTCP (dotted line) in DMF and (b) absorption spectra of polymer TCP-C_{60} (solid line), TCP/TCP-C_{60} (dashed line), and TCP/ZnTCP (dotted line) corrected by the absorption of the indium tin oxide (ITO) electrode.

of TCP. Below 400 nm, the absorption of the TCP-C_{60} dyad is higher than that of TCP due to a contribution of the C_{60} moiety. Therefore, both chromophores retain their individual identities in the ground state.[7]

The absorption spectra of the polymeric films on ITO electrodes are shown in Figure 3b. Spectra were corrected taking into account the absorption of the ITO electrode. These films showed the typical Soret band at ~440 nm and the Q bands between 515 and 650 nm, characteristic of *meso*-tetraphenylporphyrin derivatives. The UV−vis spectroscopy results also confirm the electropolymerization of the porphyrin derivatives on the ITO electrodes. In the films, the porphyrin units showed the Soret and Q bands, similar to the electronic transitions observed for the corresponding tetrapyrrolic macrocycle in solution. However, the bands of porphyrins were broader and shifted in comparison with those of the monomeric porphyrin in DMF. The maximum of the Soret band of porphyrin derivatives showed a ~10 nm bathochromic shift with respect to those in solution. Similar behavior was previously observed for the electrogenerated film of porphyrin derivatives containing *N*,*N*-diphenylaminophenyl or carbazoyl substituents.[10,11] These facts indicate the presence of interaction between porphyrins in the hyperbranched film structure.

Photosensitized Decomposition of ABMM. The detection of $O_2(^1\Delta_g)$ in water was carried out using the salt of anthracene derivative ABMM as a molecular probe, which forms 9,10-endoperoxide product (ABMM-O_2).[13] Also, we compared the results of the films with that photosensitized by $TPPS^{4-}$, as a reference. This anionic photosensitizer was chosen to avoid electrostatic interaction with ABMM.[13] Semilogarithmic plots describing the progress of the reaction for ABMM are shown in Figure 4. ABMM decomposition was

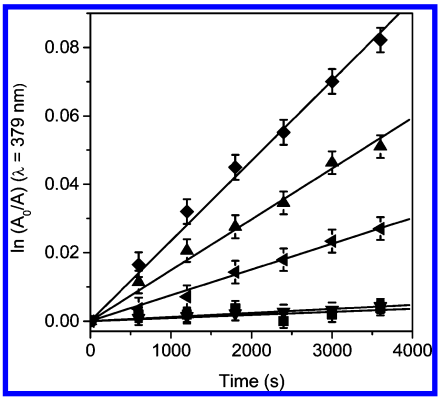

Figure 4. First-order plots for the photooxidation of ABMM (35 μM) photosensitized by TCP-C_{60} (▲), TCP/TCP-C_{60} (◀), and TCP/ZnTCP (▼) polymers on ITO electrodes, ITO electrode (■) and $TPPS^{4-}$ (◆) in water (A^{Soret} = 0.1, λ_{irr} = 455−800 nm). Values represent mean ± standard deviation of three separate experiments.

not detected in the presence of the ITO electrode without the films. From the first-order kinetic plots, the values of the observed rate constant (k_{obs}^{ABMM}) were calculated. The results are summarized in Table 1. As can be observed, a high value of reaction rate was found for ABMM decomposition photosensitized by the TCP-C_{60} film. Also, appreciable photooxidation was mediated by the TCP/TCP-C_{60} film. A higher value of ABMM photooxidation was found for the reaction photosensitized by $TPPS^{4-}$ in solution. It is known that the $TPPS^{4-}$ presents an efficient photodynamic effect in water, with a $O_2(^1\Delta_g)$ quantum yield of 0.74.[19] However, the photodecomposition of the anthracene derivative mediated by the TCP-C_{60} film was about half of that obtained for the anionic porphyrin in water. In contrast, a lower value of k_{obs}^{ABMM} was obtained using the TCP/ZnTCP film. It was previously demonstrated that the electrochemical generated heterojunction in the ITO/free-base porphyrin/Zn(II) porphyrin configuration was efficient in the generation of photoinduced charge separation states in which the Zn(II) porphyrin acts as a donor for the free-base porphyrin.[12] However, a fast recombination of the photogenerated charges was found due to the presence of the Zn(II) porphyrin in the outer layer. This effect can produce a decrease in the photodynamic activity of the TMP/ZnTMP film.

Photosensitized Reduction of NBT. The reduction of NBT to diformazan was used to detect the formation of $O_2^{\bullet-}$ in the presence of NADH. Under aerobic conditions, the photosensitized decomposition of NBT occurred mainly through a type I photoreaction process.[14] The increase of diformazan absorption at λ = 600 nm was examined as a function of time after irradiation of the samples in water. Typical results are shown in Figure S4 for the reaction photosensitized by the TCP-C_{60} film. As shown in Figure 5, the reduction of NBT by $O_2^{\bullet-}$ was not detected in the photoirradiated samples using the ITO electrode or without films/ITO electrodes. Comparing the films, a higher photodynamic activity was found in the presence of the TCP-C_{60} film. Also, decomposition of NBT was obtained using the TCP/TCP-C_{60} film. However, a very small effect was found

DOI: 10.1021/acs.est.5b01407
Environ. Sci. Technol. 2015, 49, 7456−7463

Table 1. Kinetic Parameters for the Photooxidation Reaction of ABMM (k_{obs}^{ABMM}) and Trp (k_{obs}^{Trp}) in Water

photosensitizer	k_{obs}^{ABMM} (s^{-1})	$k_{obs}^{film}/k_{obs}^{TPPS^{4-}}$ [a]	k_{obs}^{Trp} (s^{-1})	$k_{obs}^{film}/k_{obs}^{TPPS^{4-}}$ [b]
TCP-C_{60} film	$(1.33 \pm 0.06) \times 10^{-5}$	0.58	$(2.59 \pm 0.05) \times 10^{-5}$	0.90
TCP/TCP-C_{60} film	$(0.78 \pm 0.04) \times 10^{-5}$	0.34	$(1.91 \pm 0.03) \times 10^{-5}$	0.66
TCP/ZnTCP film	$(0.12 \pm 0.01) \times 10^{-5}$	0.05	$(0.88 \pm 0.05) \times 10^{-5}$	0.31
$TPPS^{4-}$	$(2.28 \pm 0.09) \times 10^{-5}$	1.00	$(2.87 \pm 0.03) \times 10^{-5}$	1.00

[a]Ratio of ABMM photooxidation. [b]Ratio of Trp photooxidation, A^{Soret} = 0.1, λ_{irr} = 455−800 nm.

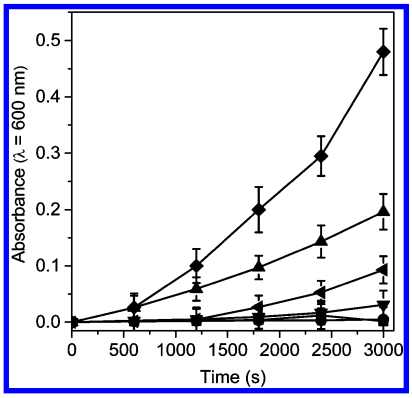

Figure 5. Time course of $O_2^{\bullet-}$ generation detected as an increase in the absorption at 600 nm by the NBT method. Samples containing NBT (0.2 mM) and NADH (0.5 mM) were photosensitized by TCP-C_{60} (▲), TCP/TCP-C_{60} (◀), and TCP/ZnTCP (▼) polymers on ITO electrodes, ITO electrode (■) and $TPPS^{4-}$ (◆) in water (A^{Soret} = 0.1, λ_{irr} = 455−800 nm). Control: NBT and NADH (●). Values represent mean ± standard deviation of three separate experiments.

with the TCP/ZnTCP film. Also, decomposition of NBT was also found in the presence of $TPPS^{4-}$ dissolved in water solution. Therefore, the TCP-C_{60} film was the more active surface to photosensitize the production of diformazan. Although, $O_2(^1\Delta_g)$ can be generated by a photoexcited photosensitizer triplet state, it was observed that $O_2^{\bullet-}$ can also be generated especially in the presence of NADH.[15]

Photooxidation of Trp. The amino acid Trp can be efficiently photodecomposed by both type I and type II reaction mechanisms.[13] Also, it can be a potential target of the photodynamic action induced by the films. Photosensitized decomposition of Trp by films was studied in water. As can be observed in Figure 6, the photooxidation of Trp showed first-order kinetics with respect to the amino acid concentration. The values of the k_{obs}^{Trp} for Trp decomposition were calculated from the plots in Figure 6. The results are shown in Table 1. A higher value of Trp decomposition was found using the TCP-C_{60} film as photosensitizer with respect to the other films. This value is similar to that found for $TPPS^{4-}$ in solution. Also, a high photooxidation rate was obtained using the TCP/TCP-C_{60} film. Also in this case, a low photodynamic activity was observed using the TCP/ZnTCP film. In the TCP/ZnTCP film, tetrapyrrolic macrocycle is directly involved in the formation of the polymer. Besides the rapid recombination of charges discussed above, relaxation processes in the polymeric network compete with the excited triplet state, decreasing the photodynamic activity. In contrast, the films bearing TCP-C_{60} have fullerene units that are attached to the polymer by a pyrrolidine ring. Thus, after visible light irradiation fullerene C_{60} can also produce efficiently ROS.

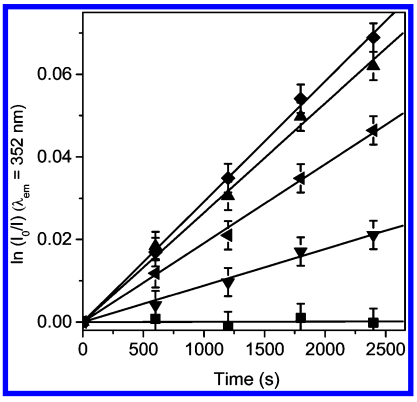

Figure 6. First-order plots for the photooxidation of Trp (20 μM) photosensitized by TCP-C_{60} (▲), TCP/TCP-C_{60} (◀), and TCP/ZnTCP (▼) polymers on ITO electrodes, ITO electrode (■) and $TPPS^{4-}$ (◆) in water (A^{Soret} = 0.1, λ_{irr} = 455−800 nm). Values represent mean ± standard deviation of three separate experiments.

As can be observed in Table 1, the rations $k_{obs}^{film}/k_{obs}^{TPPS^{4-}}$ increase for the decomposition of Trp mediated by the films in comparison with those of ABMM in water. In particular, high values were obtained when the Trp decomposition was photosensitized by the films bearing fullerenes. These results are not in agreement with the $O_2(^1\Delta_g)$ production observed using photooxidation of ABMM. Therefore, an electron transfer pathway may also be contributing, together with type II photoprocess, to Trp decomposition in water.

The network of porphyrin in the TCP-C_{60} film absorbs the visible light acting as antenna and producing energy transfer to fullerene C_{60} or the photoinduced charge-separated state. Also, the triplet excited state of fullerene ($^3C_{60}$*) can interact with ground state molecular oxygen to form ROS. This process can occur by energy transfer from the $^3C_{60}$* to produce $O_2(^1\Delta_g)$ or by electron transfer to form $O_2^{\bullet-}$. It is known that fullerenes are extremely efficient $O_2(^1\Delta_g)$ generators with a quantum yield that is near unity.[7] On the other hand, fullerenes can be reduced to C_{60} radical anion ($C_{60}^{\bullet-}$) by electron transfer.[8] Consequently, the $^3C_{60}$* or $C_{60}^{\bullet-}$ can transfer an electron to molecular oxygen producing $O_2^{\bullet-}$. The electron transfer type of reaction mainly takes place in a polar medium and in the incidence of reducing agents, such as NADH. Thus, in this film both main photochemical reaction types can be competing to produce ROS.

Photosensitized Inactivation of Bacteria. The photodynamic action induced by the polymeric films was compared *in vitro* to inactivate *S. aureus* cells. First, photoinactivation of *S. aureus* was investigated depositing a drop with the cells on the polymeric films. This antibiotic drop-test can be used to inactivate bacterial cells that contaminate a surface. Thus, 250 μL of PBS containing ~1×10^4 cells was located on polymeric films, and the plates were irradiated with visible light. Figure 7 shows the survival of bacterial cells after different irradiation times. Control experiments indicated that the viability of *S. aureus* was unaffected by light irradiation on glass or kept in the dark on the films for 60 min (results not shown). Therefore,

DOI: 10.1021/acs.est.5b01407
Environ. Sci. Technol. 2015, 49, 7456−7463

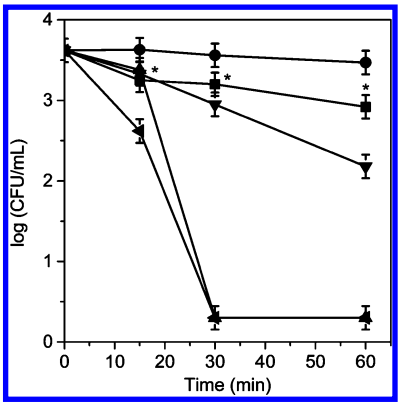

Figure 7. Survival curves of *S. aureus* cells (~10^4 CFU/mL) depositing a drop (250 μL) with the cells on the TCP-C_{60} (▲), TCP/TCP-C_{60} (◀), and TCP/ZnTCP (A^{Soret} = 0.3) (▼) polymers on ITO electrodes and ITO electrode (■). Cells were exposed to visible light for different irradiation times; A^{Soret} = 0.1 for all photosensitizer, except where indicated. Control: cells irradiated on glass (●). Values represent mean ± standard deviation of three separate experiments (*p < 0.05, compared with control).

the inactivation of *S. aureus* cells observed after irradiation was produced by the photosensitization effect of the polymeric films. After 30 min irradiation, no colony formation was detected using both polymers containing the dyad (TCP-C_{60} or TCP/TCP-C_{60} films, A^{Soret} = 0.1). This reduction represents about 99.97% decrease of cell survival, showing that the combination of visible light and polymeric films with the dyad are appropriated surfaces to photoinactivate *S. aureus*. In contrast, a low photoinactivation activity was observed with the diporphyrin TCP/ZnTCP polymeric film even using a higher absorption of 0.3 at the Soret band. Therefore, the films bearing TCP-C_{60} layers could be used to form antibacterial surfaces activated by visible light.

On the other hand, the photoinactivation activities of the polymeric films were examined against *S. aureus* cells suspensions in PBS, using small square surface parts. Thus, two polymeric surfaces (0.3 × 0.3 = 0.09 cm^2) were placed inside of the cell suspension containing ~10^4 CFU/mL and irradiated with visible light for different periods. The results are shown in Figure 8a. No toxicity was observed in untreated cells or cells in the presence of the surfaces kept in the dark (results not shown). As can be observed in Figure 8a, the microorganisms were photoinactivated when the cultures in the presence of the polymeric films were exposed to visible light. The TCP/TCP-C_{60} film exhibited a photosensitizing activity causing a 2 log decrease of *S. aureus* survival after 30 min of irradiation. A similar result was obtained with the TCP-C_{60} film but using a shorter irradiation (20 min). Furthermore, an irradiation of 30 min of the cell suspensions with this film produced a decrease of 3.5 log, which was about 99.96% of cell photoinactivation. Therefore, PDI mediated by the TCP-C_{60} polymeric film was more effective than by the TCP/TCP-C_{60} film. As previously observed, a lower activity was found using the TCP/ZnTCP film (A^{Soret} = 0.1) in comparison with those of films containing the TCP-C_{60} dyad. In this condition, the photoinactivation produced by TCP/ZnTCP was similar to that of the ITO electrode without films. However, when a surface with TCP/ZnTCP layers was prepared with absorption of 0.8 at the Soret band, it induced a 3.5 log decrease in *S. aureus* survival after 30 min irradiation.

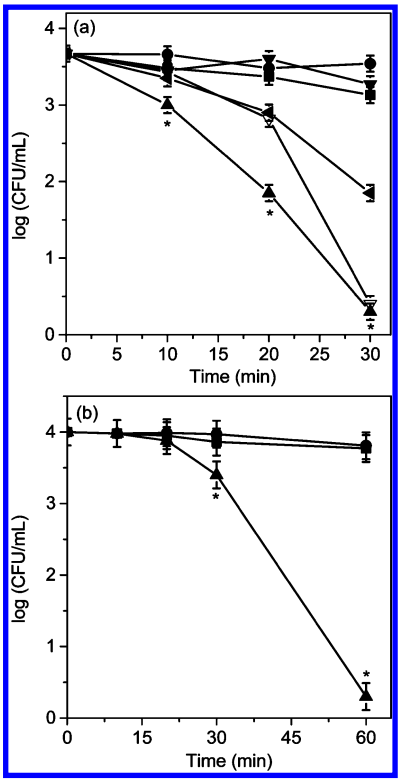

Figure 8. Survival curves of (a) *S. aureus* cell suspensions (~10^4 CFU/mL) in PBS photosensitized by TCP-C_{60} (▲), TCP/TCP-C_{60} (◀), TCP/ZnTCP (▼), and TCP/ZnTCP (A^{Soret} = 0.8) (▽) polymers on ITO electrodes and ITO electrode (■) and (b) *E. coli* cell suspensions (~10^4 CFU/mL) in PBS photosensitized by TCP-C_{60} (▲) and ITO electrode (■). Cells were exposed to visible light for different irradiation times; A^{Soret} = 0.1 for all photosensitizer, except where indicated. Control: cells untreated with the photosensitizer and irradiated (●). Values represent mean ± standard deviation of three separate experiments (*p < 0.05, compared with control).

It is known that Gram-positive bacteria are more easily inactivated by PDI than Gram-negative ones.[3] Therefore, to evaluate the efficiency of the TCP-C_{60} film in a Gram-negative bacterium, experiments were carried out with *E. coli* cells (Figure 8b). In the presence of the film, a decrease of 0.7 log in the cell viability was obtained for cells irradiated with visible light for 30 min. The outer membrane of Gram-negative bacteria forms a permeability barrier between the cell and the surrounding medium, leading to restrict the penetration of ROS.[3] Thus, to obtain about a 4 log decrease in the cell viability, it was necessary 60 min irradiation. These results represent a value greater than 99.98% of cell inactivation.

In all experiments, the TCP-C_{60} polymeric film could be reused at least three times with similar results. After treatment, the absorption spectroscopic analysis showed that the cell suspensions were not contaminated with photosensitizers that were used to form the films. On the other hand, we try to use the TCP film in PDI experiments. However, this film is not stable, and it is detached from the ITO surface in aqueous medium.

In previous studies, regenerated cellulose impregnated with 5,10,15,20-tetrakis(*N*-methylpyridinium)porphyrin tetra-*p*-tosylate showed photobactericidal activity against *S. aureus* and *E. coli*.[20] The mechanisms of the microbicidal effect were considered to be direct cell damage by $O_2(^1\Delta_g)$.[21] A photodisinfection reactor was constructed as a model for a

DOI: 10.1021/acs.est.5b01407
Environ. Sci. Technol. 2015, 49, 7456−7463

large-scale water-flow system.[22] A significant photokilling of *E. coli* was observed using the zinc(II) phthalocyanine tetrasulfonic acid/chitosan membrane as the photosensitizing surface. Cellulose laurate esters films were prepared in the presence of protoporphyrin IX.[23] Moreover, pyridinium porphyrinic chloroacetyl cellulose chlorides were obtained from chloroacetyl cellulose esters and monopyridyltritolylporphyrin.[24] These plastic films showed photobactericidal activity against *S. aureus* and *E. coli* bacteria. Also, films were formed by electrochemical polymerization of 5,10,15,20-tetra(4-*N*,*N*-diphenylaminophenyl)porphyrin and its complex with Pd(II) on ITO electrodes.[25] These films exhibit a photosensitizing activity against *E. coli* and *C. albicans* cells. On the other hand, a series of low symmetry phthalocyanine complexes supported on a polymer fiber presented antimicrobial photoinhibition activities against *S. aureus*.[26] Moreover, low symmetry lead(II) pyridyloxyphthalocyanine (PbTpyPc) and its quaternized form (PbTepyPc) were synthesized and incorporated into electrospun polystyrene fiber. PbTpyPc and PbTepyPc within the fiber matrix were employed for the photoinactivation of *E. coli* in the presence of light.[27]

In the present investigation, the polymeric films surfaces were irradiated with visible light to photoinactivate bacteria. Thus, both chromophores in the TCP-C_{60} dyad can be excited, and a contribution of the C_{60} moiety can be implicated in the inactivation of the microorganisms because the fullerene C_{60} structures are not directly involved in the formation of the polymer. It is known that fullerene C_{60} derivatives are effective photosensitizers to inactivate microorganisms.[15] Also, fullerenes are more photostable compared with tetrapyrroles. They are particularly effective at mediating type I photochemical mechanisms as opposed to the type II generation of $O_2(^1\Delta_g)$ that dominates other photosensitizers. Previous results showed that the electrochemical generated polymeric heterojunctions between free-base porphyrins and C_{60} films are able to produce photoinduced charge separated states.[12,18] Deposition of a fullerene C_{60} layer on top of the porphyrin based electropolymers showed that the electrons were separated in the direction of the external surface, while the holes were located in the porphyrin internal surface.[18] Therefore, the capacity of the polymerized dyad to generate a charge-separated state on exposure to light could be contributing to inactivate microorganisms through generation of ROS.

POTENTIAL APPLICATIONS

The hospital environment is commonly contaminated with potential pathogens that pose a risk of cross-transmission to patients.[6] In particular, *S. aureus* can survive for a long time on environmental surfaces and can be transmitted to patients via healthcare workers or the environment. In practice, manual cleaning of complex environments is difficult. Thus, novel approaches to help maintain aseptic conditions are required. This investigation presents the first example of a convenient procedure to obtain films of the porphyrin-fullerene C_{60} dyad by an electrogenerated polymer of porphyrin containing carbazoyl groups. PDI *in vitro* studies indicated that the TCP-C_{60} film is an effective surface to produce a photocytotoxic effect in bacteria. Therefore, the TCP-C_{60} film is a promising surface architecture with potential applications in microbial cell photoinactivation. As a final remark, this film has potential applications as follows: a) antibacterial surfaces activated by visible light, for example, to control microbial proliferation and maintain aseptic conditions on surfaces involved in healthcare [In particular, dental offices could benefit from such a procedure.] and b) disinfection of microbes in aqueous media. The main advantages of heterogenic eradication of microorganisms using antibacterial surfaces are that they can be easily and quickly removed from the media after cell inactivation, avoiding permanent photodynamic effects. Also, photosensitizers can be recovered and recycled from the irradiated water, producing minimal environmental pollution.

ASSOCIATED CONTENT

Supporting Information

Additional synthetic procedure of ZnTCP and figures of CV responses of electropolymerized bilayers, polymer chemical structure, photograph and microscope image of the TCP-C_{60} film on ITO, and absorption spectra changes of NBT after different irradiation times. The Supporting Information is available free of charge on the ACS Publications website at DOI: 10.1021/acs.est.5b01407.

AUTHOR INFORMATION

Corresponding Author

*Phone: 54 358 4676157. Fax: 54 358 4676233. E-mail: edurantini@exa.unrc.edu.ar.

Notes

The authors declare no competing financial interest.

ACKNOWLEDGMENTS

The authors are grateful to CONICET (PIP 112-201101-00256), SECYT UNRC (PPI 18/C400), and ANPCYT (PICT 0714/12) for financial support. M.B.S., M.E.M., M.G., L.O., and E.N.D. are Scientific Members of CONICET. M.B.B., J.D., M.B.S., and N.S.G. thank CONICET for research fellowships.

REFERENCES

(1) Theuretzbacher, U. Global antibacterial resistance: the never-ending story. *J. Global Antimicrob. Resist.* **2013**, *1*, 63−69.

(2) Nigam, A.; Gupta, D.; Sharma, A. Treatment of infectious disease: beyond antibiotics. *Microbiol. Res.* **2014**, *169*, 643−651.

(3) Alves, E.; Faustino, M. A.; Neves, M. G. P. M. S.; Cunha, A.; Tome, J.; Almeida, A. An insight on bacterial cellular targets of photodynamic inactivation. *Fut. Med. Chem.* **2014**, *6*, 141−164.

(4) Noimark, S.; Dunnill, C. W.; Parkin, I. P. Shining light on materials-A self-sterilising revolution. *Adv. Drug Delivery Rev.* **2013**, *65*, 570−580.

(5) Page, K.; Wilson, M.; Parkin, I. P. Antimicrobial surfaces and their potential in reducing the role of the inanimate environment in the incidence of hospital acquired infections. *J. Mater. Chem.* **2009**, *19*, 3819−3831.

(6) Creamer, E.; Shore, A. C.; Deasy, E. C.; Galvin, S.; Dolan, A.; Walley, N.; McHugh, S.; Fitzgerald-Hughes, D.; Sullivan, D. J.; Cunney, R.; Coleman, D. C.; Humphreys, H. Air and surface contamination patterns of meticillin-resistant *Staphylococcus aureus* on eight acute hospital wards. *J. Hosp. Infect.* **2014**, *86*, 201−208.

(7) Ballatore, M. B.; Spesia, M. B.; Milanesio, M. E.; Durantini, E. N. Synthesis, spectroscopic properties and photodynamic activity of porphyrin-fullerene C_{60} dyads with application in the photodynamic inactivation of *Staphylococcus aureus*. *Eur. J. Med. Chem.* **2014**, *83*, 685−694.

(8) Milanesio, M. E.; Alvarez, M. G.; Rivarola, V.; Silber, J. J.; Durantini, E. N. Porphyrin-fullerene C_{60} dyads with high ability to form photoinduced charge-separated state as novel sensitizers for photodynamic therapy. *Photochem. Photobiol.* **2005**, *81*, 891−897.

(9) Moor, K. J.; Kim, J.-H. Simple synthetic method toward solid supported C_{60} visible light- activated photocatalysts. *Environ. Sci. Technol.* **2014**, *48*, 2785−2791.

DOI: 10.1021/acs.est.5b01407
Environ. Sci. Technol. 2015, 49, 7456−7463

(10) Durantini, J.; Otero, L.; Funes, M.; Durantini, E. N.; Fungo, F.; Gervaldo, M. Electrochemical oxidation-induced polymerization of 5,10,15,20-tetrakis[3-(N-ethylcarbazoyl)]porphyrin. Formation and characterization of a novel electroactive porphyrin thin film. *Electrochim. Acta* **2011**, *56*, 4126−4134.
(11) Durantini, J.; Morales, G. M.; Santo, M.; Funes, M.; Durantini, E. N.; Fungo, F.; Dittrich, T.; Otero, L.; Gervaldo, M. Synthesis and characterization of porphyrin electrochromic and photovoltaic electropolymers. *Org. Electron.* **2012**, *13*, 604−614.
(12) Suarez, M. B.; Durantini, J.; Santo, M.; Otero, L.; Milanesio, M. E.; Durantini, E.; Gervaldo, M. Electrochemical generation of porphyrin-porphyrin and porphyrin-C_{60} polymeric photoactive organic heterojunctions. *Electrochim. Acta* **2014**, *133*, 399−406.
(13) Mora, S. J.; Milanesio, M. E.; Durantini, E. N. Spectroscopic and photodynamic properties of 5,10,15,20-tetrakis[4-(3-N,N-dimethylaminopropoxy)phenyl]porphyrin and its tetracationic derivative in different media. *J. Photochem. Photobiol., A* **2013**, *270*, 75−84.
(14) Yamakoshi, Y.; Umezawa, N.; Ryu, A.; Arakane, K.; Miyata, N.; Goda, Y.; Masumizu, T.; Nagano, T. Active oxygen species generated from photoexcited fullerene (C_{60}) as potential medicines: $O_2^{-\cdot}$ versus $^1O_2$. *J. Am. Chem. Soc.* **2003**, *125*, 12803−12809.
(15) Milanesio, M. E.; Spesia, M. B.; Cormick, M. P.; Durantini, E. N. Mechanistic studies on the photodynamic effect induced by a dicationic fullerene C_{60} derivative on *Escherichia coli* and *Candida albicans* cells. *Photodiagn. Photodyn. Ther.* **2013**, *10*, 320−327.
(16) Gervaldo, M.; Fungo, F.; Durantini, E. N.; Silber, J. J.; Sereno, L. E.; Otero, L. Carboxyphenyl metalloporphyrins as photosensitizers of semiconductor film electrodes. A study of the effect of different central metals. *J. Phys. Chem. B* **2005**, *109*, 20953−20962.
(17) Fungo, F.; Otero, L.; Borsarelli, C. D.; Durantini, E. N.; Silber, J. J.; Sereno, L. Photocurrent generation in thin SnO_2 nanocrystalline semiconductor film electrodes from photoinduced charge-separation state in porphyrin-C_{60} dyad. *J. Phys. Chem. B* **2002**, *106*, 4070−4078.
(18) Durantini, J.; Suarez, M. B.; Santo, M.; Durantini, E.; Dittrich, T.; Otero, L.; Gervaldo, M. Photoinduced charge separation in organic-organic heterojunctions based on porphyrin electropolymers. Spectral and time dependent surface photovoltage study. *J. Phys. Chem. C* **2015**, *119*, 4044−4051.
(19) Gottfried, V.; Peled, D.; Winkelman, J. W.; Kimel, S. Photosensitizers in organized media: singlet oxygen production and spectral properties. *Photochem. Photobiol.* **1988**, *48*, 157−163.
(20) Bonnett, R.; Buckley, D. G.; Burrow, T.; Galia, A. B. B.; Saville, B.; Songca, S. P. Photobactericidal materials based on porphyrins and phthalocyanines. *J. Mater. Chem.* **1993**, *3*, 323−324.
(21) Bonnett, R.; Evans, R. L.; Galia, A. B. B. Immobilized photosensitizers: photosensitizer films with microbicidal effects. *Proc. Soc. Photo-Opt. Instrum. Eng.* **1997**, *3191*, 79−88.
(22) Bonnett, R.; Krysteva, M. A.; Lalov, I. G.; Artarsky, S. V. Water disinfection using photosensitizers immobilized on chitosan. *Water Res.* **2006**, *40*, 1269−1275.
(23) Krouit, M.; Granet, R.; Branland, P.; Verneuil, B.; Krausz, P. New photoantimicrobial films composed of porphyrinated lipophilic cellulose esters. *Bioorg. Med. Chem. Lett.* **2006**, *16*, 1651−1655.
(24) Krouit, M.; Granet, R.; Krausz, P. Photobactericidal plastic films based on cellulose esterified by chloroacetate and a cationic porphyrin. *Bioorg. Med. Chem.* **2008**, *16*, 10091−10097.
(25) Funes, M. D.; Caminos, D. A.; Alvarez, M. G.; Fungo, F.; Otero, L. A.; Durantini, E. N. Photodynamic properties and photoantimicrobial action of electrochemically generated porphyrin polymeric films. *Environ. Sci. Technol.* **2009**, *43*, 902−908.
(26) Masilela, N.; Kleyi, P.; Tshentu, Z.; Priniotakis, G.; Westbroek, P.; Nyokong, T. Photodynamic inactivation of *Staphylococcus aureus* using low symmetrically substituted phthalocyanines supported on a polystyrene polymer fiber. *Dyes Pigm.* **2013**, *96*, 500−508.
(27) Osifeko, O. L.; Nyokong, T. Applications of lead phthalocyanines embedded in electrospun fibers for the photoinactivation of *Escherichia coli* in water. *Dyes Pigm.* **2014**, *111*, 8−15.

DOI: 10.1021/acs.est.5b01407
Environ. Sci. Technol. 2015, 49, 7456−7463